References and Notes

1. W. Baumeister, R. Grimm, J. Walz, *Trends Cell Biol.* **9**, 81 (1999).
2. B. F. McEwen, J. Frank, *Curr. Opin. Neurobiol.* **11**, 594 (2001).
3. R. G. Hart, *Science* **159**, 1464 (1968).
4. Reviewed in A. J. Koster *et al.*, *J. Struct. Biol.* **120**, 276 (1997).
5. Reviewed in B. F. McEwen, M. Marko, *J. Histochem. Cytochem.* **49**, 553 (2001).
6. K. Dierksen, D. Typke, R. Hegerl, A. J. Koster, W. Baumeister, *Ultramicroscopy* **40**, 71 (1992).
7. K. Dierksen, D. Typke, R. Hegerl, W. Baumeister, *Ultramicroscopy* **49**, 109 (1993).
8. R. Hegerl, W. Hoppe, *Z. Naturforsch. Sect. A Phys. Sci.* **31**, 1717 (1976).
9. B. F. McEwen, K. H. Downing, R. M. Glaeser, *Ultramicroscopy* **60**, 357 (1995).
10. R. Grimm *et al.*, *Biophys. J.* **72**, 482 (1997).
11. R. Grimm *et al.*, *Biophys. J.* **74**, 1031 (1998).
12. D. Nicastro, A. S. Frangakis, D. Typke, W. Baumeister, *J. Struct. Biol.* **129**, 48 (2000).
13. R. Grimm, A. J. Koster, U. Ziese, D. Typke, W. Baumeister, *J. Microsc.* **183**, 60 (1996).
14. Materials and methods are available as supporting material on *Science* Online.
15. A. Muller-Taubenberger *et al.*, *EMBO J.* **20**, 6772 (2001).
16. D. Voges, P. Zwickl, W. Baumeister, *Annu. Rev. Biochem.* **68**, 1015 (1999).
17. J. M. Peters, Z. Cejka, J. R. Harris, J. A. Kleinschmidt, W. Baumeister, *J. Mol. Biol.* **234**, 932 (1993).
18. M. Rechsteiner, L. Hoffman, W. Dubiel, *J. Biol. Chem.* **268**, 6065 (1993).
19. H. Holzl *et al.*, *J. Cell Biol.* **150**, 119 (2000).
20. M. H. Glickman *et al.*, *Cell* **94**, 615 (1998).
21. J. E. Heuser, M. W. Kirschner, *J. Cell Biol.* **86**, 212 (1980).
22. T. M. Svitkina, A. B. Verkhovsky, K. M. McQuade, G. G. Borisy, *J. Cell Biol.* **139**, 397 (1997).
23. L. A. Flanagan *et al.*, *J. Cell Biol.* **155**, 511 (2001).
24. G. P. Resch, K. N. Goldie, A. Krebs, A. Hoenger, J. V. Small, *J. Cell Sci.* **115**, 1877 (2002).
25. Reviewed in J. E. Bear, M. Krause, F. B. Gertler, *Curr. Opin. Cell Biol.* **13**, 158 (2001).
26. Reviewed in D. Pantaloni, C. Le Clainche, M. F. Carlier, *Science* **292**, 1502 (2001).
27. Reviewed in J. V. Small, T. Stradal, E. Vignal, K. Rottner, *Trends Cell Biol.* **12**, 112 (2002).
28. C. Hug *et al.*, *Cell* **81**, 591 (1995).
29. M. Haugwitz, A. A. Noegel, J. Karakesisoglou, M. Schleicher, *Cell* **79**, 303 (1994).
30. J. Niewöhner, I. Weber, M. Maniak, A. Muller-Taubenberger, G. Gerisch, *J. Cell Biol.* **138**, 349 (1997).
31. M. Tsujioka, L. M. Machesky, S. L. Cole, K. Yahata, K. Inouye, *Curr. Biol.* **9**, 389 (1999).
32. E. L. de Hostos, *Trends Cell Biol.* **9**, 345 (1999).
33. R. Insall *et al.*, *Cell Motil. Cytoskel.* **50**, 115 (2001).
34. T. P. Stossel *et al.*, *Nature Rev. Mol. Cell. Biol.* **2**, 138 (2001).
35. E. Lee, K. Pang, D. A. Knecht, *Biochim. Biophys. Acta* **1525**, 217 (2001).
36. J. L. Podolski, T. L. Steck, *J. Biol. Chem.* **265**, 1312 (1990).
37. R. D. Mullins, J. A. Heuser, T. D. Pollard, *Proc. Natl. Acad. Sci. U.S.A.* **95**, 6181 (1998).
38. H. N. Higgs, T. D. Pollard, *Annu. Rev. Biochem.* **70**, 649 (2001).
39. M. Schliwa, *Nature Rev. Mol. Cell. Biol.* **3**, 291 (2002).
40. Reviewed in R. Grünewald, O. Medalia, A. Gross, A. C. Steven, W. Baumeister, *Biophys. Chem.*, in press.
41. J. Böhm *et al.*, *Proc. Natl. Acad. Sci. U.S.A.* **97**, 14245 (2000).
42. A. S. Frangakis *et al.*, *Proc. Natl. Acad. Sci. U.S.A.* **99**, 14153 (2002).
43. J. M. Plitzko *et al.*, *Trends Biotechnol.* **20**, S40 (2002).
44. J. Walz *et al.*, *J. Struct. Biol.* **121**, 19 (1998).

45. O.M. thanks the European Commission for a Marie Curie fellowship. I.W. was supported by a grant from the Deutsche Forschungsgemeinschaft (SFB 266 to G.G.). We thank J. Köhler for the movie and A. C. Steven for critical reading of the manuscript.

Supporting Online Material
www.sciencemag.org/cgi/content/full/298/5596/1209/DC1
Materials and Methods
Movie S1

16 July 2002; accepted 9 September 2002

Superconductivity in Dense Lithium

Viktor V. Struzhkin,[1]* Mikhail I. Eremets,[2] Wei Gan,[1,3] Ho-kwang Mao,[1] Russell J. Hemley[1]

Superconductivity in compressed lithium is observed by magnetic susceptibility and electrical resistivity measurements. A superconducting critical temperature (T_c) is found ranging from 9 to 16 kelvin at 23 to 80 gigapascals. The pressure dependence of T_c suggests multiple phase transitions, consistent with theoretical predictions and reported x-ray diffraction results. The observed values for T_c are much lower than those theoretically predicted, indicating that more sophisticated theoretical treatments similar to those proposed for metallic hydrogen may be required to understand superconductivity in dense phases of lithium.

Lithium is considered the simplest metal: it is the lightest of the alkali metals, and under normal pressure-temperature conditions its properties are well described within a nearly free electron model. The two inner core electrons effectively shield the nucleus, inhibiting electron-ion attraction and leaving the outer electrons to move freely within the ion lattice. Because the valence electron is so delocalized, lithium is a metal with high conductivity and it assumes a highly symmetric body-centered cubic (bcc) structure. Recent studies show that under pressure, however, this simplicity changes radically. Theoretical predictions (*1*) suggest that lithium may undergo several structural transitions, possibly leading to a "paired-atom" phase with low symmetry and near-insulating properties. Though this prediction is the antithesis of the intuitive expectation that pressure favors high-symmetry crystal structures with metallic properties, recent x-ray diffraction studies reveal a structure similar to the predicted paired structure (*2*). Near 39 GPa, lithium transforms to a cubic polymorph with 16 atoms per unit cell (cI16), a recently discovered structure unique to lithium (*2*). Additionally, a minimum in the electronic density of states close to the Fermi energy suggests near-insulator behavior in the paired structure.

The ambient-pressure phase of Li at low temperature is not bcc but rather a closed packed rhombohedral 9R structure (*3*). Under ambient pressure, no sign of superconductivity in lithium has been detected down to 4 mK (*4*). However, it is predicted that lithium's structural changes under pressure may have large effects on possible superconductivity in the material (*1*, *5*). Explicit calculations (*6*) suggest that T_c may reach a maximum of 60 to 80 K in the cI16 phase. An early resistivity experiment had indicated a possible superconducting transition in lithium (*7*) at 7 K and higher pressures; however, the experiment was inconclusive due to the lack of magnetic signature of the transition. Similar experiments, performed recently with a diamond anvil cell to higher pressures, confirmed a resistance drop and established a dependence of the drop on external magnetic field but still lacked the magnetic susceptibility measurement necessary for proving superconductivity (*8*). Because of the difficulties in studying the material under pressure [e.g., sample containment and reactivity (*2*, *9*)], it is essential to apply a variety of probes of the compressed sample. For superconductivity, this includes the combination of magnetic (*10*) and electrical (*11*) techniques.

Magnetic susceptibility measurements were performed in two experiments (*12*). The temperature scan at 28 GPa in the second run is shown in Fig. 1. We used a Nb sample placed in the compensating coil at ambient pressure as a reference in this experiment. The signal from Nb is superimposed in phase with the background; the signal from Li is opposite in phase from that of the background. The compensating and signal coils are connected in opposition; thus, the signal from Li has actually the same phase as that from Nb and, therefore, indubitably corresponds to the superconducting transition. We observed

[1]Geophysical Laboratory, Carnegie Institution of Washington, 5251 Broad Branch Road, N.W., Washington, DC 20015, USA. [2]Max Planck Institut für Chemie, Postfach 3060, 55020 Mainz, Germany. [3]Thomas S. Wootton High School, Rockville, MD 20850, USA.

*To whom correspondence should be addressed. E-mail: struzhkin@gl.ciw.edu

a similar phase relation for the background and the superconducting signal in our experiments on sulfur to 230 GPa (*13*). Magnetic susceptibility measurements at selected pressures are shown in the right panel in Fig. 2.

Complementary resistivity measurements were carried out as follows. Resistivity measurements could not be performed in gaskets made of cubic BN mixed with epoxy used in our previous experiments (*11*) because of the possibility of chemical reactions between Li and epoxy. To isolate the Li sample from the gasket, we used a ring of 100-μm inner diameter and 250-μm outer diameter made of a NiCr(Al) gasket preindented to a thickness of 20 μm. Beveled diamond anvils with 600-μm bevels and 200-μm flat culets were used. The resistivity was measured by the four-probe technique, with a signal from the sample shunted by the NiCr(Al) ring. The contribution from the sample, however, was high enough (10%) for easy detection of the superconducting transition. We found that the resistivity response was broadened if measuring currents ~100 μA or higher were used to detect the transition; this occurs because the measuring current exceeded the critical superconducting current I_c close to the transition. Distinct superconducting steps were clearly seen when a 20-μA measuring current was used (Fig. 2).

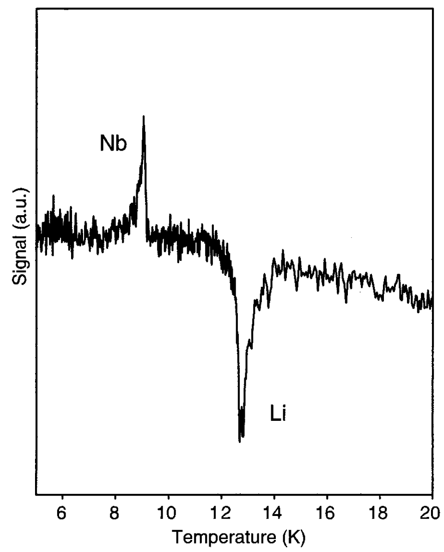

Fig. 1. Magnetic susceptibility signal at 28 GPa. The signal from Li is superimposed on a paramagnetic background with the opposite sign. The signal from Nb in the compensating coil at ambient pressure has an inverted phase and it is superimposed on the background additively.

The pressure dependence of the T_c for Li is shown in Fig. 3. T_c rapidly increases with pressure from 9 K at 23 GPa to 16 K at 33 GPa, and above that pressure it drops down to 10.5 K at 40 GPa. These changes in T_c indicate the possibility of structural phase transitions. According to the resistivity data, T_c increases to above 16 K in the range 43 to 46 GPa and remains almost constant to at least 60 GPa. A T_c in the vicinity of 20 K has been observed in resistivity measurements involving magnetic quenching in a pressure range 40 to 50 GPa by Shimizu (*8*). At 66 GPa the resistivity signal shows very broad response below 15 K. Further increase in pressure to 80 GPa shifts the onset of the superconducting step down to 11 K. The observed changes in T_c with pressure are qualitatively compatible with the variety of predicted low-symmetry phases at high pressure (*1*, *2*); however, detailed x-ray diffraction measurements at low temperatures are required to make a direct comparison with our results. We plot phase boundaries consistent with our data in Fig. 3. The available T_c data suggest possible phase boundaries around 33 to 36 GPa, 40 to 50 GPa, and 66 to 80 GPa. The first two boundaries correlate well with x-ray diffraction data (*2*) at higher temperatures; the last one may be a transition to yet another phase, possibly the paired Cmca phase predicted theoretically (*1*).

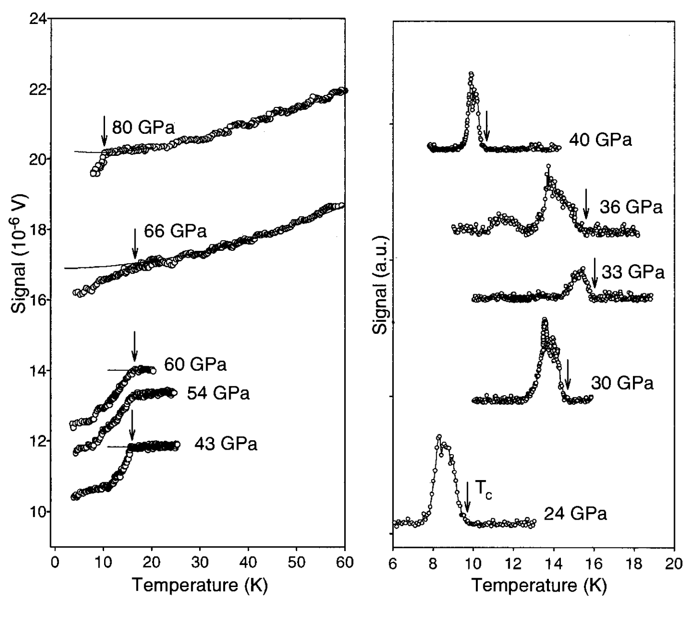

Fig. 2. Temperature scans at high pressure. (Left) Resistivity measurements. The signal is measured using a four-probe technique. The absolute value of the signal at the lock-in amplifier input is plotted with a measuring current of 20 μA at 38 Hz. We used a 1:30 transformer between our sample and lock-in amplifier to improve the signal-to-noise ratio, so the actual signal is about 30 times less than shown in the figure. T_c is identified as the onset of the transition. The very broad and featureless response at 66 GPa may be due to the mixture of two phases. (Right) Magnetic susceptibility measurements. The background signal is subtracted (*13*), and the T_c is estimated from the onset of the transition.

We now compare our pressure dependence of T_c with theoretical predictions. The T_c was calculated to increase dramatically in the face-centered cubic (fcc) phase to 50 to 70 K just before the transition to hR1 (and subsequently to the cI16 phase) near 40 GPa, staying nearly constant and very high (60 to 80 K) in the cI16 phase from 40 to at least 80 GPa (*6*). Our results are consistent with the steep increase of T_c below 30 GPa as occurring in the fcc phase, but with a much lower T_c than predicted. The drop in T_c to 10.5 K at 40 GPa may indicate that a transition to yet another phase occurs in the narrow pressure range (38 to 43 GPa), similar to the intermediate hexagonal phase observed by x-ray diffraction in the same pressure range [carried out below 200 K (*2*)]. Above 43 GPa, the experimental T_c values stay nearly constant at 16 K. Assuming the cI16 phase is stable in this pressure range (*2*), the theoretical prediction (*6*) for the T_c is much higher than is experimentally observed. The possibility of spin fluctuations reducing T_c was discussed in [(*6*) and references therein]. The difference may also arise from the possibility of large Coulomb corrections due to electron-electron repulsion (*14*). In general, this question can be addressed by studying the isotope effect on T_c. A reduced isotope effect indicates large values of μ^* (the repulsive electron-electron interaction), larger than is found for most simple metals. Notably, it has been argued (*15*) that a reduced isotope effect documented in the recently discovered high-temperature superconductor MgB_2 indicates the large values of μ^* in this material.

The present results add to the recent find-

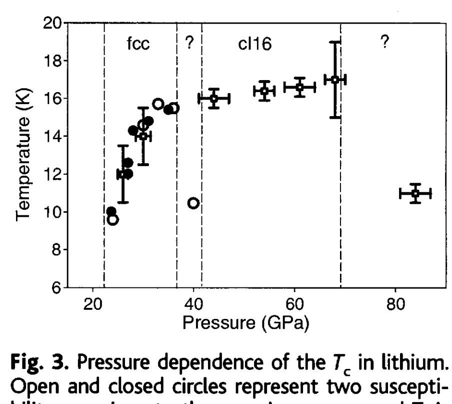

Fig. 3. Pressure dependence of the T_c in lithium. Open and closed circles represent two susceptibility experiments; the error in pressure and T_c is less than or equal to the symbol size. The resistivity data are shown as squares. The dashed lines represent possible phase boundaries. Further experimental details can be found in (*12*).

ings regarding the emerging complexity of putatively simple metals under pressure (1, 2, 5, 16, 17). Despite its apparent deviations from a textbook "simple metal," Li remains an ideal candidate for further theoretical understanding of the origin of this complexity because of its low atomic number. Although there is a possibility that the low-temperature phases are distinct from those considered in (6), the discrepancies between theory and experiment may be resolved by assuming very high values of the Anderson-Morel Coulomb pseudopotential μ^* or by invoking spin fluctuation effects (6). The first possibility may require a full treatment of electrons and ions on the same footing similar to the approach proposed by Richardson and Ashcroft (14). Such a treatment is likely to be very important for understanding the behavior (including possible high-temperature superconductivity) in the predicted metallic phases of hydrogen at higher pressures (14, 18, 19). This study shows the power of pressure as a variable in uncovering phenomena in condensed matter, findings made possible by continued advances in experimental high-pressure techniques.

References and Notes

1. J. B. Neaton, N. W. Ashcroft, *Nature* **400**, 141 (2000).
2. M. Hanfland, K. Syassen, N. E. Christensen, D. L. Novikov, *Nature* **408**, 174 (2000).
3. A. W. Overhauser, *Phys. Rev. Lett.* **53**, 64 (1984).
4. K. M. Lang *et al.*, *J. Low Temp. Phys.* **114**, 445 (1999).
5. N. W. Ashcroft, in *Proceedings of the International School of Physics "Enrico Fermi,"* R. J. Hemley, G. Chiarotti, M. Bernasconi, L. Ulivi, Eds., vol. **CXLVII**, in press.
6. N. E. Christensen, D. L. Novikov, *Phys. Rev. Lett.* **86**, 1861 (2001).
7. T. H. Lin, K. J. Dunn, *Phys. Rev. B* **33**, 807 (1986).
8. K. Shimizu, private communication.
9. V. V. Struzhkin, R. J. Hemley, H. K. Mao, *Bull. Am. Phys. Soc.* **44**, 1489 (1999).
10. Yu. A. Timofeev, V. V. Struzhkin, R. J. Hemley, H. K. Mao, E. Gregoryanz, *Rev. Sci. Instrum.* **73**, 371 (2002).
11. M. I. Eremets, V. V. Struzhkin, H. K. Mao, R. J. Hemley, *Science* **293**, 272 (2001).
12. Materials and methods are available as supporting material on *Science* Online.
13. E. Gregoryanz *et al.*, *Phys. Rev. B* **65**, 064504 (2002).
14. C. F. Richardson, N. W. Ashcroft, *Phys. Rev. B*, **55**, 15130 (1997).
15. D. G. Hinks, H. Claus, J. D. Jorgensen, *Nature* **411**, 457 (2001).
16. R. J. Nelmes, M. I. McMahon, J. S. Loveday, S. Rekhi, *Phys. Rev. Lett.* **88**, 155503 (2002).
17. J. S. Tse, private communication.
18. C. F. Richardson, N. W. Ashcroft, *Phys. Rev. Lett*, **78**, 118 (1997).
19. K. Moulopoulos, N.W. Ashcroft, *Phys. Rev. B* **59**, 12309 (1999).

20. Supported by the DOE grant #DEFG02-02ER45955, the NSF (DMR-0205899), and the W. M. Keck Foundation. W.G. acknowledges support from REU Site for Undergraduate Research Training in Geoscience (NSF EAR-0097569), W. G. Minarik, and S. B. Shirey. We thank J. Schilling and J. Tse for useful comments and discussions.

Supporting Online Material

www.sciencemag.org/cgi/content/full/1078535/DC1
Materials and Methods

18 September 2002; accepted 7 October 2002
Published online 17 October 2002;
10.1126/science.1078535
Include this information when citing this paper.

REPORTS

Fatigue Failure in Polysilicon Not Due to Simple Stress Corrosion Cracking

H. Kahn, R. Ballarini,* J. J. Bellante, A. H. Heuer*

In the absence of a corrosive environment, brittle materials such as silicon should be immune to cyclic fatigue. However, fatigue effects are well known in micrometer-sized polycrystalline silicon (polysilicon) samples tested in air. To investigate the origins of this phenomenon in polysilicon, we developed a fixed-grip fracture mechanics microspecimen but could find no evidence of static stress corrosion cracking. The environmental sensitivity of the fatigue resistance was also investigated under cyclic loading. For low-cycle fatigue, the behavior is independent of the ambient conditions, whether air or vacuum, but is strongly influenced by the ratio of compressive to tensile stresses experienced during each cycle. The fatigue damage most likely originates from contact stresses at processing-related surface asperities; subcritical crack growth then ensues during further cyclic loading. The lower far-field stresses involved in high-cycle fatigue induce reduced levels of fatigue damage. Under these conditions, a corrosive ambient such as laboratory air exacerbates the fatigue process. Without cyclic loading, polysilicon does not undergo stress corrosion cracking.

Silicon is a "fully" brittle material at room temperature. In the absence of hydrostatic confining pressures to suppress fracture, silicon displays no stress-induced dislocation activity under ambient conditions, even under high stresses, and undergoes no stress-induced phase transformations, except at extremely high pressures (1). In addition, stress corrosion cracking (2) has not been conclusively detected in silicon (3, 4). We thus do not expect silicon to display any time-dependent cracking (neither crack initiation nor crack extension) when subjected to monotonic or cyclic loading conditions. Experimental results, however, have shown otherwise. Precracked micrometer-sized specimens of both single-crystal (4) and polycrystalline silicon (polysilicon) (5) exhibit crack extension when subjected to cyclic fatigue loading. Crack initiation and growth have also been observed in micrometer-sized silicon specimens without precracks under fatigue loading (6–11). Both single-crystal silicon (6, 7) and polysilicon (8–11) have been studied. Most of the investigations (6–10) used equal tension/compression cycling, for a load ratio $R = -1$. (The load ratio R is the ratio of the minimum stress to the maximum stress in the cycle; tension is taken as positive and compression as negative.) Fatigue has also been observed in zero/tension stress cycling tests ($R = 0$) (11). Muhlstein *et al.* (9, 10) have attributed the limited lifetime to "reaction-layer fatigue." This fatigue mechanism involves the surface oxide (12) on the silicon undergoing damage through stress corrosion cracking; the oxide is postulated to thicken because of continued chemical reaction with the ambient, and the cracks lengthen until the stress intensity factor reaches the critical fracture toughness K_{IC} (Eq. 1), whereupon catastrophic crack propagation ensues. Bagdahn *et al.* (11), however, showed that the lifetime of polysilicon specimens subjected to tensile fatigue loading was dependent only on the number of cycles and not on the cycling frequency.

In fact, stress corrosion is not a prerequisite for fatigue behavior in brittle materials. Suresh (13) showed that brittle ceramics display crack initiation and propagation at notches under compression/compression fatigue loading. He attributed the fatigue to confined damage at the notch tip during compression loading, which generates tensile stresses and microcracking upon unloading. Further, Wiederhorn *et al.* (14) reported temperature-dependent subcritical crack growth in a variety of inorganic glasses subjected to constant tensile loads in vacuum (10^{-2} Pa).

For our investigation, the test structure shown in Fig. 1 was used to investigate the static (constant load) stress corrosion of polysilicon in micrometer-sized specimens. The fracture mechanics microspecimen, a doubly clamped beam with a residual tensile stress and containing a sharp precrack produced by a Vickers microindent, was fabricated with standard micromachining techniques (15). Upon release of the structure, the residual tensile stress in the film produced a nearly uniform tensile stress in the doubly clamped beam and, in turn, a well-defined stress intensity at the crack tip. The residual stress in the film was measured with microstrain gauges, which were micromachined on the same substrate and placed near the test devices. We

Case Western Reserve University, 10900 Euclid Avenue, Cleveland, OH 44106–7204, USA.

*To whom correspondence should be addressed: E-mail: rxb7@po.cwru.edu (R.B.); ahh@po.cwru.edu (A.H.H.)